Differ Equ Dyn Syst (January–July 2019) 27(1–3):249–276
https://doi.org/10.1007/s12591-017-0402-6

ORIGINAL RESEARCH

Another Mechanism to Control Invasive Species and Population Explosion: "Ecological" Damping Continued

Rana D. Parshad[1] · **Guangming Yao**[1] · **Wen Li**[1,2]

Published online: 16 November 2017

Abstract The control of nonnative species is a central problem in spatial ecology. Data on the invasive Burmese python (*Python bivittatus*) in the Florida everglades, show an exponential increase in python population, which have resulted in local prey populations reducing severely (Dorcas et al. in Proc Natl Acad Sci 109:2418–2422, 2012). This is exacerbated by the inability to harvest pythons by law, in Everglades National Park, where their concentration is extremely high. We consider a two species predator–prey model with Beddington–DeAngelis functional response, and show that it blows up in finite time, thus mimicking an "exploding" python population. Given current government policy that requires complete protection of species in national parks, we investigate novel alternative population control measures that promote efficient eco-system engineering. We establish such measures are feasible in our setting by rigorously proving boundary damping effects. That is we show that an exploding population in a region can be controlled, *solely* via manipulation of the boundary, such as effective corridor design. Detailed numerical simulations are performed to justify our analytical results.

Keywords Predator prey model · Finite time blow-up · Radial basis function · Mixed boundary conditions

Mathematics Subject Classification Primary · 35B44 · 35K57 · 65M70; Secondary · 92D25

✉ Wen Li
liw2@clarkson.edu

Rana D. Parshad
rparshad@clarkson.edu

1 Department of Mathematics, Clarkson University, Potsdam, NY 13699, USA

2 College of Big Data Science, Taiyuan University of Technology, Taiyuan 030024, China

Introduction

Background

An *invasive* species is formally defined as any species capable of propagating itself in a nonnative environment and thus establishing a self-sustained population. In the United States damages caused by invasive species to agriculture, forests, fisheries and businesses, have been estimated to be $120 billion a year [1]. To quote from [2]: "Invasive species are a greater threat to native biodiversity than pollution, harvest, and disease combined." Therefore understanding and subsequently attenuating the spread of invasive species is an important and practical problem [3–9]. In many ecosystems around the world various invasive species have *already* established, such as the Burmese python invasion in the Florida everglades [10]. Thus, a very relevant problem in spatial ecology is the actual control of such established invasive populations.

Eradication is optimal, but often eco-system managers are satisfied if targeted invasive species can be kept to low/manageable levels. Current eradication efforts for many invasive species usually involve chemical treatment, local harvesting, dewatering, ichthyocides, or a suitable combination [11]. Unfortunately, many of these methods are known to negatively impact native fauna [11], are expensive, and are *not* reversible. A notable example is when the United States Geological Survey (USGS) attempted a *mass scale* poisoning of fish, to prevent the invasive Asian carp from entering the Chicago Sanitary and Ship Canal, so as to protect the fishing interests of the region. Unfortunately after the poison had taken effect, biologists found *only one Asian carp* among the thousands of dead fish [12]. Similarly, in 2016, in an effort to control the mosquito population that carries the Zika virus, an aerial pesticide was used. This inadvertently resulted in the death of *millions* of honeybees [13]. The most current control measures have focused on shifting the sex ratio of invasive aquatic populations [14]. Therein adding individuals containing two Y chromosomes (YY females) to an invasive population to skew the sex ratio of subsequent generations to contain an increasing number of males (i.e., fewer and fewer females in each generation). The gradual reduction in females may lead to eventual extinction of the population. Such methods are reversible and have the advantage of targeting a specific invasive species [15]. Recent work has also focused on using pheromone based techniques [16], in the context of the invasive cane toad. The tadpoles of cane toads eliminate competition by locating and eating new eggs, via chemical cues from the eggs. Researchers have shown that using those very same cues, funnel traps in waterbodies can be used to capture and eradicate cane toad tadpoles [16].

Environmental pressures also promote population explosion. For example, the environment may turn unfavorable for the competitors or natural enemies of a species, causing the population of this species to rapidly increase unchecked or *outbreak* [17]. As an illustration, in the European Alps certain seasonal environmental conditions enable the population of the larch budmoth to become large enough to defoliate entire forests [18]. Extreme weather events for example could have both positive or negative effects on invasive species selection [19]. Thus in most ecosystems, if the density of an invasive species/pest undergoes a rapid transition to an extremely high level in population, the results can be catastrophic, both for local and nonlocal populations.

Control Mechanisms and "Ecological" Damping

One can ask what measures apart from chemical control, are available to target invasive populations. Biological control is an alternative adopted strategy to limit harmful populations

[20]. The objective of a biological control is to establish a management strategy that best controls and decreases the harmful population to healthy levels as opposed to high and risky levels. This can be done via introduction of natural enemies of the pest into the ecosystem perse. Naturally, how does one define *high* level, and further, how well does the biological control actually work, at various high levels? We have recently started investigating this question via the mathematical property of finite time blow-up [21–26].

Given a mathematical model for the population dynamics of a species, one can investigate the question of whether there is a globally (in time) existing solution, or perhaps if finite time blow-up occurs. That is,

$$\lim_{t \to T^* < \infty} \|u\|_X = \infty, \tag{1}$$

where X is a certain function space with a norm $\|\cdot\|$, u is the population density of the species in question (described by an evolution equation) that depends on time (t) as well as spatial variables ($\mathbf{x}$), and T^* is the blow-up time [27,28]. In the context of population biology finite time blow-up has been well investigated [7,29–31].

Note, we have now introduced an alternate viewpoint: finite time blow-up. This can be viewed as *mimicking* the explosive growth of an invasive species. This is formalised by equating:

$$\text{finite time blow-up} = uncontrollable \text{ and } unmanageable \text{ population level.} \tag{2}$$

Here, the blow-up time T^* is viewed as the *disaster* time, for the ecosystem.

Although populations cannot reach infinite values in finite time, they can grow rapidly [17]. For example, experimental evidence suggest that the human population may be growing hyperbolically, rather than logistically [32]. Data on the Burmese python suggests that its population is growing at least exponentially, causing severe crashes in local prey populations [10]. Our approach investigates biological control mechanisms, that attempt to lower and control the targeted population *before time* T^*. These rely on eco-friendly/grass-roots and community programs [24], and avoid classical chemical and biological control [20]. We term this as "Ecological" Damping [24]. With this approach there is no ambiguity as to what is a disastrous high level of population. Furthermore, there is a clear demarcation between the disaster occurring, or not occurring. We survey the most recent literature in this direction

- There is a potential for the predator density to blow-up/explode in finite time, for sufficiently large initial values of predator density [21,23].
- The blow-up can occur even for *small* initial values of predator densities [33].

These ideas have also been applied to model invasive populations that seem to be "exploding", under a variety of ecological scenarios. The most current findings in the literature thus far are that

- Prey refuge can prevent blow-up [24].
- Interference effects among the predators increases the propensity to blow-up [34].
- Climate induced mortality in the predator can prevent blow-up [35].
- Gestation effect in predator can prevent blow-up [25,36].

Remark 1 Conditions for the prevention of blow-up via manipulation of boundary conditions are *completely* lacking in the literature.

Remark 2 Note a similar concept of finite time consensus has been studied quite intensively in the control theory literature. Here the system under consideration will reach a consensus/agreement state in a finite/fixed time. Such methods have far reaching applications in

group hunting by predators, coordinated military decisions and actions and coordinated search and rescue procedures. For details the interested reader is referred to [37,38].

Python Explosion in the Everglades and New Mechanisms of Control

The Burmese python (*Python bivittatus*) is an invasive species of snake in the Florida everglades, whose entry into the region is mostly attributed to the exotic pet trade [1]. Data from python capture show an exponential increase in python population, which has in turn spelled doom for many native endangered species, that fall prey to the python [10]. A separate issue here is that due to current government policy, all species in National parks in the United States are protected by law and so harvesting of pythons in the actual park area is deemed illegal [39]. Furthermore the large area of the park, the rich source of prey there, and low detectability of the python, are all factors causing the python population to grow unchecked. Thus one is led to consider alternate control measures. One possibility is to attempt to use mechanisms at the boundary of the park (given that the interior is protected by law). Also, how does one convert such a novel control method into sound management practice? The heart of the matter mathematically, is to understand and investigate the effect of various boundary conditions. This is discussed next.

In our approach to investigate population explosion problems and their subsequent control, we have considered only Dirichlet or Neumann boundary conditions earlier [24,34]. It is important to briefly glean over boundary conditions, as they appear in reaction diffusion problems in spatial ecology. One is referred to [40] for a thorough treatment. Typically one has, a partial differential equation model for a state variable $u(x,t)$ (usually representing the concentration or density of a species), with $x \in \Omega$, where Ω is the physical domain of interest. One treats the general boundary condition $a(x)\nabla u \cdot n + b(x)u = 0$ on $\partial\Omega$. If $b(x) = 0$, we have pure no-flux boundary condition, indicating no individuals cross the boundary, and the boundary is essentially a perfect barrier. If $a(x) = 0$ then we have the so called lethal/hostile/absorbing boundary, where individuals are annihilated/absorbed as they meet the boundary. Typically the mixed boundary condition requires $a(x), b(x) \neq 0$. If $a(x), b(x) > 0$, then we have a situation where some individuals from the interior of the domain *cross* the boundary when they meet it, thus moving outside the domain. This is the situation we are most interested in.

Setting $a(x), b(x) > 0$, is purely mathematical. In reality, when a species in the interior of Ω meets the physical boundary $\partial\Omega$, it may or may not be the easiest thing to move across it. Thus we first have to establish that in theory such a boundary condition can indeed provide a damping effect in our setting. Next we link this mechanism to the design of more efficient pathways and corridors [41], so that the species in question will *indeed* be able to cross over. Our contributions in the current manuscript are the following:

- We investigate a two species predator–prey model, where the predator population, has the potential to blow-up in finite time. We investigate this phenomenon first under purely Neumann boundary conditions, showing blow-up is possible via Theorems 2.2 and 2.3.
- We show that blow up is possible under mixed (in particular Robin type) boundary conditions, for large initial data, via Theorem 2.4.
- However, we show that the mixed (in particular Robin type) boundary conditions can also provide a "damping" effect. That is, global existence of finite population is possible with the Robin type boundary condition with small initial data, via Theorem 2.5.
- In particular we derive conditions via Corollary 1 such that the two species model (5)–(6) posed with Neumann boundary conditions blows up in finite time, whilst the two

Table 1 List of functions and parameters used in the model with their physical meaning

Symbols	Meaning
u	Prey
v	Predator
r	Growth rate of prey u
K	Carrying capacity of prey u
ω	Maximum rate of per capita removal of prey u
d	Measure of refuge provided by the environment for the prey u
D	Predator interference
c	Growth rate of v via sexual reproduction.
ω_1	Maximum rate of per capita removal of predator species v
D_1	Alternate food available to predator v

All parameters are assumed to be positive constants

species model (5)–(6) with mixed boundary conditions (with the same initial conditions and parameters) is bounded for all time.

- Turing instability is impossible in this model system, for *any* parameter regime, via Theorem 2.6.
- Detailed numerics are performed on the PDE system on square and circular domains to justify our analytical results, and explore various parameter/data regimes. See "Numerical simulations".

Model Formulation

The predator–prey ODE model from the recent work of Upadhyay et al. [42] is first considered

$$\frac{du}{dt} = ru(1-u/K) - \frac{\omega uv}{D+du+v}, \tag{3}$$

$$\frac{dv}{dt} = cv^2 - \frac{\omega_1 v^2}{u+D_1}, \tag{4}$$

where $r, \omega, D, d, c, \omega_1, D_1$ are model parameters, v denotes a generalist predator population as a function of time t, depredating on a prey population u. The functional response of the predator is of Beddington–DeAngelis type [43]. This response assumes that the predators *interfere* with each others feeding.

The parameter definitions are given in Table 1:

Definition 1.1 (*Generalist Predator*) A generalist predator is a hunting organism that feeds on a wide variety of prey.

Definition 1.2 (*Interference*) Mutual interference is defined as the behavioral interactions among feeding organisms, that reduce the time that each individual spends obtaining food, or the amount of food each individual consumes.

Interference occurs commonly among predators when prey is scarce, or when the predator population is at high density. The reader is referred to [29,34,36,44–49] for further details. Note that the classical Holling type II response function, for a population of predators say

given by v, depredating on a prey population u, would take the form $f(u) = u/(u+d)$, with d as a parameter. That is the predator v has a purely prey dependent functional response. Interference is often modeled via the Beddington–DeAngelis response [43] which takes the form $f(u, v) = u/(v + b_1u + d)$. The constant b_1 is then the interference parameter, and the response changes due to the assumption that high predator density, should also affect their feeding rate. Intuitively, at higher values of v, $u/(v + b_1u + d)$ is small, and the predator feeds less, because there is more time spent as the various predators interfere with each other, in their search for prey [49]. Note, the Beddington–DeAngelis formulation assumes that handling and searching are mutually exclusive, that is predators handling prey will *not* interfere with those searching for prey. Interference occurs most commonly where the amount of food is scarce, or when the population of feeding organisms is large [47]. Note, food chain models incorporating mutual interference appear a fair bit in the literature [44,45,48].

The predator is modeled according to the modified Leslie–Gower scheme. In this formulation the functional response of the predator *is not similar* to that of its prey. The generalist predator population grows quadratically as cv^2, signifying population growth is directly proportional to the product of males and females ($v \times v = v^2$). The population decays due to intraspecies competition as $-(\omega_1/(u + D_1))v^2$. Thus if the u population is large, v has enough prey, and so the competition coefficient $\omega_1/(u + D_1)$, is small. On the other hand if the u population is small, v has lack of sufficient prey, and so the competition coefficient $\omega_1/(u + D_1)$, is large, inducing greater competition amongst the predators v. The D_1 shows that v is a true generalist predator, and can switch to alternate prey, in case its favorite prey u goes extinct. The ODE model is referred to as ODE system.

Remark 3 We would like to remark that we consider the autonomous problem, and all the parameters in our setting are pure constants, not time dependent functions. Many times the non-autonomous problem is also considered, when there is a physical motivation that these intrinsic rates could be time dependent. For example in population ecology mating rates could be seasonal [35]. Also, random environmental fluctuations have lead many researchers to consider stochastic rates, such as in the setting of random weather driven events. For example, Acacia mearnsii is a shallow-rooted tree introduced in Yunnan province, in China. Significant decline was observed for this species relative to the regions native trees, during the drought of 2009–2010. Another example where random climatic fluctuation stops invasive species population growth, is the destruction of shell beds in the Yellow River in China, by extreme storms. The interested reader is referred to [35,50,51] for recent results in these directions. However in our setting the nonautonomous problem is outside the scope of the current research.

The spatially explicit form of the above ODE model can be considered, if species are allowed to freely diffuse in search of food, mates etc. Thus, the ODE system can be extended to two-dimensional space, we obtain the following PDE model:

$$u_t = D_u\Delta u + ru(1 - u/K) - \frac{\omega uv}{D + du + v}, \tag{5}$$

$$v_t = D_v\Delta v + cv^2 - \frac{\omega_1 v^2}{u + D_1}. \tag{6}$$

The model (5)–(6) is referred as PDE system.

Due to the large python population in the Florida everglades, and the diminishing source of prey, model system (5)–(6) seems ecologically appropriate to model the python situation in the glades.

Preliminaries

We now present various notations and definitions that will be used frequently. The usual norms in the spaces $\mathbb{L}^p(\Omega)$ and $\mathbb{L}^\infty(\Omega)$ respectively denoted by

$$\|u\|_p^p = \frac{1}{|\Omega|}\int_\Omega |x(s)|^p\, ds,$$
$$\|u\|_\infty = \max_{s\in\Omega} |x(s)|\,.$$

Existence of Local Solution

It is well-known [27] under the "regularizing effect principle" to prove global existence of solutions to (5)–(6) , it suffices to derive uniform estimates on the L^p norms of the reaction terms on $[0, T_{\max}]$ for some $p > n/2$, where n is the spatial dimension of the domain Ω, where $T_{\max}$ denotes the eventual blowing-up time in $\mathbb{L}^\infty(\Omega)$. The following local existence result is well-known [27].

Lemma 2.1 *The system* (5)–(6) *admits a unique, classical solution* (u, v) *on* $[0, T_{\max}] \times \Omega$. *If* $T_{\max} < \infty$ *then*

$$\lim_{t\to T_{\max}} \{\|u(t,\cdot)\|_\infty + \|v(t,.)\|_\infty\} = \infty. \tag{7}$$

Proof Since the reaction terms are continuously differentiable in the positive octant, then for any initial data in $\mathbb{L}^p(\Omega)$, $p \in (1, +\infty)$, it is easy to check directly their Lipschitz continuity on bounded subsets of the domain of a fractional power of the operator $I_2\,(D_u, D_v)^t\,\Delta$, where I_2 the two dimensional identity matrix, Δ is the Laplacian operator and $()^t$ denotes the transposition. □

Remark 4 In the estimates that follow, C, C_1, C_2 are generic constants. They can change in value from line to line, and sometimes within the same line, if so required.

Finite Time Blow Up for Large Initial Data

We first show that the solution v to (6) can blow up in finite time for large initial data. In particular we state the following theorem:

Theorem 2.2 *Consider the two species model* (5)–(6). *The solution to* (6), $v(x, t)$, *blows up in finite time. That is* $\lim_{t\to T^*<\infty} ||v(x,.)||_\infty = \infty$ *as long as the initial data* $(u_0(x), v_0(x))$ *are large enough.*

Proof Consider ODE version of (5)–(6), with positive initial conditions. By integrating (4) we obtain

$$v = \frac{1}{\frac{1}{v_0} - ct + \omega_1 \int_0^t \frac{ds}{u+D_1}}.$$

Our goal, following [23], is to show that, for u_0 chosen sufficiently large, via the continuity of the solution component u on a the local interval of existence following classical theory

[27], there exists a $\delta > 0$ such that

$$\begin{aligned}\psi(t) &= \frac{1}{v_0} - ct + \omega_1 \int_0^t \frac{ds}{u + D_1} \\ &= \frac{1}{v_0} + \left[-c + \frac{\omega_1}{t}\int_0^t \frac{ds}{u + D_1}\right] t \\ &< \frac{1}{v_0} - \frac{c}{2}t, \quad \text{for all } t \in (0, \delta). \end{aligned} \tag{8}$$

Now for v_0 chosen sufficiently large, then we can find $T^* \in (0, \delta)$ such that

$$\frac{1}{v_0} - \frac{c}{2}T^* = 0,$$

which gives us by application of the mean value theorem, the existence of some $T^{**} \in (0, \delta)$, $T^{**} < T^*$, s.t $\psi(T^{**}) = 0$. This implies $v(t)$ the solution of (6), blows-up in finite time, at $t = T^{**}$. Via standard comparison, the result for the PDE follows, proving the theorem. □

Sufficient Condition on Data for Blow Up

Theorem 2.3 *Consider the two species PDE model (5)–(6), for any choice of parameters, and a $\delta_1 > 0$, such that $c > \delta_1$. If a given initial condition (u_0, v_0) satisfies*

$$\frac{\omega_1}{\delta_1} < ||v_0||_\infty \ln\left(\frac{||u_0||_\infty}{\frac{\omega_1}{c-\delta_1} - D_1}\right) \tag{9}$$

then the solution to (6), v, will blow-up in finite time, that is $\lim_{t \to T^* < \infty} ||v||_\infty = \infty$, where the blow-up time $T^* \leq 1/\delta_1 ||v_0||_\infty$.

Proof Consider the equation for the predator

$$\frac{dv}{dt} = \left(c - \frac{\omega_1}{u + D_1}\right) v^2.$$

In the event that $c > \frac{\omega_1}{D_1}$, blow-up is trivial. If $c < \frac{\omega}{D_1}$, blow-up is far from obvious. However still possible, under certain sufficiency conditions on the initial data. Suppose

$$\left(c - \frac{\omega_1}{u + D_1}\right) > \delta_1 > 0.$$

Then in the ODE case, v will blow-up in finite time in comparison with

$$\frac{dv}{dt} = \delta_1 v^2.$$

In the PDE case, we require $\min_{x \in \Omega} u(x, t) \geq \frac{\omega_1}{c-\delta_1} - D_1$, and then blow up is obvious in comparison with

$$v_t = \Delta v + \delta_1 v^2.$$

Note this is sufficient, not necessary. To see how this can be guaranteed we make estimates on the prey u, via comparing it to a sub-solution

$$\begin{aligned} u_t &= D_u\Delta u + ru(1-u/K) - \frac{\omega uv}{D+du+v} \\ &> D_u\Delta u + ru(1-u/K) - \frac{\omega uv}{v} \\ &= D_u\Delta u + ru(1-u/K) - \omega u. \end{aligned}$$

Note, here we use the positivity of the predator v and prey u and the fact that $\frac{\omega uv}{D+du+v} < \frac{\omega uv}{v}$, and so $-\frac{\omega uv}{D+du+v} > -\frac{\omega uv}{v}$. Thus, via standard theory if $r > \omega$, u will converge uniformly to the steady state $u^* = K(1-\frac{\omega}{r})$. Now if $K(1-\frac{\omega}{r}) > \left(\frac{\omega_1}{c} - D_1\right)$, then u will eventually rise above the level $\left(\frac{\omega_1}{c} - D_1\right)$ point-wise, making blow up a certainty. However, it might turn out that $K(1-\frac{\omega}{r}) < \left(\frac{\omega_1}{c} - D_1\right)$. In this case we compare with the sub-solution

$$u_t = D_u\Delta u + ru(1-u/K) - \frac{\omega uv}{D+du+v} > D_u\Delta u - \omega u.$$

via classical theory we have that

$$u > u_0 e^{-(C+\omega_1)t}.$$

This estimate holds point-wise. Thus in order to have blow up, we require that

$$u > u_0 e^{-(C+\omega_1)t} > \frac{\omega_1}{c-\delta_1} - D_1.$$

Equivalently,

$$\ln\left(\frac{||u_0||_\infty}{\frac{\omega_1}{c-\delta_1} - D_1}\right) > t(C+\omega_1).$$

Note that

$$v_t = \Delta v + cv^2$$

blows-up at time $T^* = 1/c||v_0||_\infty$. Thus, if we choose initial data such that

$$\ln\left(\frac{||u_0||_\infty}{\frac{\omega_1}{c-\delta_1} - D_1}\right)\frac{1}{(C+\omega_1)} > t > T^* = \frac{1}{c||v_0||_\infty},$$

then the above inequality guarantees that the min of u will remain above the critical level $\frac{\omega_1}{c-\delta_1} - D_1$, for sufficiently long enough time, for v to blow-up. This yields that as long as the following holds

$$||v_0||_\infty \ln\left(\frac{||u_0||_\infty}{\frac{\omega_1}{c-\delta_1} - D_1}\right) > \frac{(C+\omega_1)}{c},$$

then v will blow up in finite time. This proves the theorem. □

Blow Up with Mixed Boundary Conditions

Here we derive sufficient conditions under which blow up is possible with mixed boundary conditions. We state the following theorem:

Theorem 2.4 *Consider the two species model (5)–(6) posed with mixed boundary conditions that is* $a\nabla v \cdot n + bv = 0|_{\partial\Omega}$. *If* $c > \omega$ *and* $c > \omega_1/\left(\frac{r-\omega}{r}\right)K + D_1$, *then* $v(x,t)$ *the solution to (6) blows up in finite time, that is* $\lim_{t\to T^*<\infty} ||v(x,.)||_\infty = \infty$, *as long as the initial data* $v_0(x)$ *is sufficiently large.*

Proof Again, we can compare u, with a subsolution

$$\begin{aligned} u_t &= D_u\Delta u + ru(1-u/K) - \frac{\omega uv}{D+du+v} \\ &> D_u\Delta u + ru(1-u/K) - \frac{\omega uv}{v} \\ &= D_u\Delta u + ru(1-u/K) - \omega u. \end{aligned}$$

The sub-solution that is the u^* solving $u_t = D_u\Delta u + ru(1-u/K) - \omega u$, will converge to $\left(\frac{r-\omega}{r}\right)K$ uniformly, thus after a certain transition time T_1, we must have, by comparison, that $u > \left(\frac{r-\omega}{r}\right)K$, with the estimate being true point-wise in x.

Now this implies that for $t > T_1$,

$$cv^2 - \frac{\omega_1 v^2}{u+D_1} = \left(c - \frac{\omega_1}{u+D_1}\right) > c - \frac{\omega_1}{\left(\frac{r-\omega}{r}\right)K + D_1}. \tag{10}$$

Since by assumption, we have $c > \omega_1/\left(\frac{r-\omega}{r}\right)K + D_1$, then for $t > T_1$, (6) reduces to

$$v_t = D_v\Delta v + \left(c - \frac{\omega_1}{\left(\frac{r-\omega}{r}\right)K + D_1}\right)v^2 > D_v\Delta v + \delta v^2 \tag{11}$$

$$a\nabla v \cdot n + bv = 0, \text{ on } \partial\Omega. \tag{12}$$

We thus have to analyze the above problem, and adhere to standard methods [52]. We recap a few details for the sake of completeness. We consider

$$\phi(t) = \int_\Omega v^2 dx. \tag{13}$$

One easily derives,

$$\phi'(t) \geq -3\left(\frac{b}{a}D_v\int_{\partial\Omega} v^2 ds + D_v\int_\Omega |\nabla v|^2 dx\right) + 6\int_\Omega v^3 dx = \psi(t). \tag{14}$$

It is also easily derived that

$$\psi'(t) = 6\int_\Omega (v_t)^2 dx. \tag{15}$$

Since $\psi'(t) \geq 0$, it must be that $\psi(t) \geq 0$, for $t > 0$ if $\psi(0) \geq 0$. Also it is easily seen via Cauchy-Schwartz that $[\phi'(t)]^2 \leq \phi(t)\psi'(t)$, and since $\phi'(t) \geq \psi(t)$, standard calculus yields

$$\frac{\psi'(t)}{\psi(t)} \geq \frac{3}{2}\frac{\phi'(t)}{\phi(t)} \tag{16}$$

and so integration in time yields

$$\psi(t) \geq M\phi(t)^{\frac{3}{2}}, \tag{17}$$

where $M = \psi(0)/(\phi(0))^{\frac{3}{2}}$. Now using the fact again that $\phi^{'}(t) \geq \psi(t)$, we have

$$\phi^{'}(t) \geq M\phi(t)^{\frac{3}{2}}. \tag{18}$$

Thus integration in time of the above inequality yields the finite time blow up of $\phi(t) = \int_\Omega |v|^2 dx$, for large enough initial data. □

Remark 5 Next we provide explicit estimations of $v_0(x)$ required to yield blow up. Note, as long as $M = \psi(0)/(\phi(0))^{\frac{3}{2}} \geq 0$, $\phi(t)$ will blow up in finite time. Since $\phi(0) = \int_\Omega (v_0(x))^2 dx > 0$, M will be strictly greater than 0 as long as $\psi(0) > 0$. Thus solving

$$\psi(0) = -3\left(\frac{b}{a}D_v \int_{\partial\Omega} (v_0(x))^2 ds + D_v \int_\Omega |\nabla v_0(x)|^2 dx\right) + 6\int_\Omega (v_0(x))^3 dx > 0, \tag{19}$$

we can give the following sufficient explicit estimate for the largeness of the initial data $v_0(x)$ for blow up to occur:

$$2\int_\Omega (v_0(x))^3 dx > \frac{b}{a}D_v \int_{\partial\Omega} (v_0(x))^2 ds + D_v \int_\Omega |\nabla v_0(x)|^2 dx. \tag{20}$$

We see this can be achieved by using an initial condition $v_0(x)$ large in amplitude, so that its $L^3(\Omega)$ norm will be large, whilst we can make the right hand side of the above small by choosing $D_v << 1$, as well as $b << 1$.

Next we derive sufficient conditions under which blow up can be *prevented* using mixed boundary conditions. We state the following theorem:

Theorem 2.5 *Consider the two species model (5)–(6) posed with mixed boundary conditions, that is $a\nabla v \cdot n + bv = 0$, on $\partial\Omega$. Then the $L^2(\Omega)$ norm of solutions to this model, are bounded for all time, for sufficiently small initial data.*

Proof We compare the solution of (6) to a super solution via

$$cv^2 - \frac{\omega_1 v^2}{u + D_1} = \left(c - \frac{\omega_1}{u + D_1}\right) v^2 < cv^2. \tag{21}$$

Now note

$$v_t = D_v \Delta v + \left(c - \frac{\omega_1}{u + D_1}\right) v^2 < D_v \Delta v + cv^2, \quad \text{in } \Omega \tag{22}$$

$$a\nabla v \cdot n + bv = 0, \quad \text{on } \partial\Omega. \tag{23}$$

We attempt to prove global existence for

$$v_t = D_v \Delta v + cv^2, \quad \text{in } \Omega \tag{24}$$

$$a\nabla v \cdot n + bv = 0, \quad \text{on } \partial\Omega, \tag{25}$$

because any global bound derived here, will be a bound for the v solving (6), by simple comparison. We multiply (24) by u and integrate in space on Ω, and use (25) to obtain

$$\begin{aligned} \frac{1}{2}\frac{d}{dt}\int_\Omega |v|^2 dx &= -D_v \int_{\partial\Omega} |\nabla v|^2 dx + D_v \int_{\partial\Omega} v\nabla v \cdot n ds + c\int_\Omega v^3 dx \\ &\leq -D_v \int_\Omega |\nabla v|^2 dx - D_v \frac{b}{a}\int_{\partial\Omega} |v|^2 ds + c\int_\Omega v^3 dx. \end{aligned} \tag{26}$$

Recall the Gagliardo–Nirenberg interpolation inequality [53],

$$||\phi||_{W^{k,p}(\Omega)} \leq C||\phi||^{\theta}_{W^{m,q}(\Omega)}||\phi||^{1-\theta}_{L^r(\Omega)}, \quad \text{for } \phi \in W^{m,q}(\Omega) \tag{27}$$

provided $p, q, r \geq 1, 0 \leq \theta \leq 1$, and

$$k - \frac{n}{p} \leq \theta\left(m - \frac{n}{q}\right) + (1-\theta)\frac{n}{r}, \quad \text{where } n = dim\ \Omega. \tag{28}$$

Now we consider exponents such that

$$W^{k,p}(\Omega) = L^3(\Omega),\ W^{m,q}(\Omega) = H^1(\Omega),\ L^r(\Omega) = L^2(\Omega), \tag{29}$$

so $k = 0$, $p = 3, m = 1, q = 2, r = 2, n = 2$, thus $\frac{1}{3} \leq \theta \leq 1$. Thus, choosing

$$\theta = \frac{1}{3}, \tag{30}$$

we obtain via an application of the Gagliardo–Nirenberg interpolation inequality on v solving (6)

$$||v||_3 \leq C||\nabla v||_2^{\frac{1}{3}}||v||_2^{\frac{2}{3}}. \tag{31}$$

Thus we obtain

$$||v||_3^3 \leq C||\nabla v||_2||v||_2^2. \tag{32}$$

Injecting the above into (24) we obtain

$$\begin{aligned}\frac{1}{2}\frac{d}{dt}\int_\Omega |v|^2dx &\leq -D_v\int_\Omega |\nabla v|^2dx - D_v\frac{b}{a}\int_{\partial\Omega}|v|^2ds + c\int_\Omega v^3dx\\ &\leq -D_v\int_\Omega |\nabla v|^2dx - D_v\frac{b}{a}\int_{\partial\Omega}|v|^2ds + cC\left(\int_\Omega |\nabla v|^2dx\right)^{\frac{1}{2}}\left(\int_\Omega v^2dx\right)\\ &\leq -D_v\int_\Omega |\nabla v|^2dx - D_v\frac{b}{a}\int_{\partial\Omega}|v|^2ds + D_v\int_\Omega |\nabla v|^2dx\\ &\quad + C_1\left(\int_\Omega v^2dx\right)^2. \end{aligned} \tag{33}$$

This follows via employing Young's inequality with ϵ, with $\epsilon = \sqrt{\frac{2D_v}{cC}}$. Let us call $F(t) = \int_\Omega v^2dx$, then the above entails

$$\frac{d}{dt}F(t) \leq 2C_1F(t)^2 - 2D_v\frac{b}{a}\delta_2. \tag{34}$$

where $\int_{\partial\Omega} v^2ds > \delta_2 > 0$. Integration of the above equation now yields a global solution as long as the initial data $v_0(x)$ is small enough. □

Remark 6 Next we provide explicit estimations of $v_0(x)$ required to yield a global in time solution. That is we specify in terms of model parameters how "small" $v_0(x)$ really needs to be. Note, as long as $F(0) = \int_\Omega (v_0(x))^2dx \leq 2D_v\frac{b}{a}\frac{\delta_2}{C_1}$, $F(t)$ will exist globally, in comparison to

$$\frac{d}{dt}F(t) = 2C_1F(t)^2 - 2D_v\frac{b}{a}\delta_2, \tag{35}$$

and cannot blow up in finite time. Thus solving

$$F(0) = \int_\Omega (v_0(x))^2 dx \leq 2D_v \frac{b}{a} \frac{\delta_2}{C_1}, \tag{36}$$

we can now give the following sufficient explicit estimate for the smallness of the initial data $v_0(x)$ for global in time existence:

$$\int_\Omega (v_0(x))^2 dx \leq 2D_v \frac{b}{a} \frac{\delta_2}{C_1}. \tag{37}$$

Remark 7 We would like to remark on the physical interpretation of the condition $\int_{\partial\Omega} v^2 ds > \delta_2, \forall t$, that we have used in the above proof. This follows mathematically via the positivity of v on the boundary, and the mixed boundary condition that we prescribe. Physically this implies that the density of the predator on the actual boundary is always positive, while its net flux across the boundary could be negative or positive. That is there could be predators inside the domain, leaving through the boundary on contact with it, to go outside(and this is the case if $a, b > 0$, or negative net flux) or coming into the domain from outside (and this is the case if either $a < 0, b > 0$ or $a > 0, b < 0$, or positive net flux).

Remark 8 Note if $b = 0$, then we would have $\frac{d}{dt} F(t) \leq 2C_1 F(t)^2$, and be unable to claim global existence for small data. Thus the mixed boundary condition facilitates global existence for small data.

Corollary 1 *Consider the two species model (5)–(6) posed with Neumann boundary conditions. Consider now initial conditions and a parameter set, for which the sufficiency conditions of Theorem 2.3 are met. Then the two species model (5)–(6) posed with Neumann boundary conditions, blows up in finite time. It is possible to choose $b > 0$ large enough such that the $L^2(\Omega)$ norm of solutions to the two species model (5)–(6) with the same initial conditions and parameters, with mixed boundary conditions however, that is $a\nabla v \cdot n + bv = 0$, on $\partial\Omega$, is bounded for all time.*

Proof Since the conditions of Theorem 2.3 are met we have

$$\frac{\omega_1}{\delta_1} < ||v_0||_\infty \ln\left(\frac{||u_0||_\infty}{\frac{\omega_1}{c-\delta_1} - D_1} \right). \tag{38}$$

Without loss of generality let us choose $\delta_1 = 1$, $c > 1$. We can always choose $b > 0$ (possibly $b >> 1$) such that $C||v_0||_\infty^2 \leq 2D_v \frac{b}{a} \frac{\delta_2}{C_1}$. Where the C is the optimal constant in the embedding of $L^\infty(\Omega) \hookrightarrow L^2(\Omega)$. This will entail

$$||v_0||_2^2 \leq C||v_0||_\infty^2 \leq 2D_v \frac{b}{a} \frac{\delta_2}{C_1}, \tag{39}$$

which will enforce the $L^2(\Omega)$ norm of solutions to the two species model (5)–(6) with mixed boundary conditions, to be bounded for all time, via Theorem 2.5, whilst the two species model (5)–(6) posed with Neumann boundary conditions, blows up in finite time, due to the result of Theorem 2.3. □

Turing Instability

This section shows that the Turing instability is impossible in the PDE model.

Theorem 2.6 *Consider the two species model described by (5)–(6). The nontrivial spatially homogenous steady state* (u^*, v^*) *cannot be driven unstable due to diffusion for any range of parameters.*

Proof The Jacobian evaluated at the interior steady state (u^*, v^*) is

$$J(u^*, v^*) = \begin{bmatrix} u^*\left(-\frac{r}{K} - \frac{\omega d v^*}{(D+du^*+v^*)^2}\right) & \frac{\omega u^*(D+du^*)}{(D+du^*+v^*)^2} \\ \frac{\omega_1 v^{*2}}{(u^*+D1)^2} & 0 \end{bmatrix}. \tag{40}$$

A necessary condition for Turing instability in 2-species systems is that $J_{11}|_{u^*,v^*} + J_{22}|_{u^*,v^*} < 0$, but $D_u J_{11}|_{u^*,v^*} + D_v J_{22}|_{u^*,v^*} > 0$. In our case:

$$D_u J_{11}|_{u^*,v^*} + D_v J_{22}|_{u^*,v^*} = D_u(u^*)\left(-\frac{r}{K} - \frac{\omega d v^*}{(D+du^*+v^*)^2}\right) + D_v(0) < 0$$

making the required necessary condition an impossibility. This then makes it impossible for Turing instability to occur, via classical theory [54], in our two species model described by (5)–(6). □

Numerical Simulations

In this section, we will introduce a numerical method in class of radial basis function (RBF) collocation method, the method of particular solutions, to solve the two-dimensional model (5)–(6). An radial basis function (RBF), $\phi_j(\mathbf{x})$ is a function that function's values depend only on the distance to a center point $\mathbf{x}_j$. Thus, it can be rewritten as $\phi_j(\mathbf{x}) = \phi(\|\mathbf{x}-\mathbf{x}_j\|) = \phi(r)$, where $r = \|\mathbf{x} - \mathbf{x}_j\|$. This notation indicates the numerical procedure involving RBFs in high-dimensional space will be the same as for problems in one-dimensional space, except that the distance needs to be defined differently in different dimensional spaces.

This motivates many scientists and researchers to broadly apply RBFs on solving various kinds of interpolation problems, PDE problems, and their applications in various engineering, biology, biomedical fields [55–58]. The commonly used RBFs includes Gaussian, multi-quadrics (MQ), inverse multiquadrics (IMQ), polyharmonic splines (PS), and etc. The most of the commonly used RBFs, except PS, contains a shape parameter, which usually effect the accuracy of the numerical methods tremendously. In the meanwhile there is not any effective methodology that can be used to find a suitable shape parameter for various kinds of problems.

The method of approximated particular solutions (MAPS) was first proposed by Chen et al. [59], using MQ and IMQ. Since then, the closed form particular solutions for many commonly used RBFs and differential operators have been derived [60,61]. As a result, MAPS was extended to Matérn and Gaussian RBFs and to many types of PDEs [59,62–66]. PS has rarely been used in MAPS due to its conditional positive definiteness and low accuracy, [67]. In [62], MAPS is modified so PHS can be used more effectively. In the original MAPS, integrated RBFs, so called particular solutions, are used. In the modified MAPS, an additional polynomial basis is directly added to the integrated RBFs without integration. It is remarkable that MAPS becomes extremely accurate when we use the PS kernels in the proposed method.

In this paper, we will apply PS RBF to our two-dimensional predator–prey model (5)–(6). We will first to use the implicit time-stepping scheme to discretize the time domain, and then the system of nonlinear parabolic equations becomes a system of nonlinear elliptic equations.

MAPS with PS are then applied to discretize the spatial variables at every time step. The detailed numerical procedure are briefly introduced below.

MAPS using Polyharmonic Splines

For any interested time interval, $t \in [0, T]$. We discrete the time domain by partition the time domain equally $t_n = nh$, where $n = 0, 1, 2, \ldots, N_t$, $h = T/N_t$. Then the model (5)–(6) becomes

$$\frac{u_{n+1} - u_n}{h} = D_u \Delta u_{n+1} + r u_n (1 - u_n/K) - \frac{\omega u_n v_n}{D + d u_n + v_n}, \tag{41}$$

$$\frac{v_{n+1} - v_n}{h} = D_v \Delta v_{n+1} + c v_n^2 - \frac{\omega_1 v_n^2}{u_n + D_1} \tag{42}$$

for all $\mathbf{x} \in \Omega$, where $u_n = u(\mathbf{x}, t_n)$, $u_{n+1} = u(\mathbf{x}, t_{n+1})$, $v_n = v(\mathbf{x}, t_n)$, and $v_{n+1} = v(\mathbf{x}, t_{n+1})$.

Rearrange the system, we have that

$$u_{n+1} - D_u \Delta u_{n+1} = u_n + h \left(r u_n (1 - u_n/K) - \frac{\omega u_n v_n}{D + d u_n + v_n} \right), \tag{43}$$

$$v_{n+1} - D_v \Delta v_{n+1} = v_n + h \left(+ c v_n^2 - \frac{\omega_1 v_n^2}{u_n + D_1} \right). \tag{44}$$

When $n = 0$, we are given u_n, v_n from the initial conditions. Thus, the right-hand side of the system (43)–(44) is known. We will need to solve the elliptic equations to find an approximation to u_{n+1} and to v_{n+1}. The (43)–(44) are solved simultaneously by MAPS. For our simplicity, we assume the elliptic equation of type

$$\mathbf{L} w_{n+1} = f(u_n, v_n), \tag{45}$$

with suitable boundary conditions

$$\mathbf{B} w_{n+1} = g(u_n, v_n), \tag{46}$$

where $w = [u, v]$. In two-dimensional space, the MAPS uses the integrated PS

$$\Phi(r) = \frac{r^{2m+2} \ln r}{4(m+1)^2} - \frac{r^{2m+2}}{4(m+1)^3} \tag{47}$$

where $m \in \mathbf{Z}^+$, $\Delta \Phi(r) = \phi(r) = r^{2m} \ln(r)$ with a monomial basis of the polynomial space of order m,

$$\Psi(\mathbf{x}) = x^{i-j} y^j \tag{48}$$

where $0 \le j \le l$, $0 \le l \le m$. For our simplicity, we represent the polynomial space of order m by $\mathcal{P} = \{p_1, p_2, \ldots, p_q\}$, where $q = (m+1)(m+2)/2$. Solutions to the elliptic equations can then be approximated by the function of the form

$$w(\mathbf{x}) \approx \hat{w}(\mathbf{x}) = \sum_{k=1}^{N} \alpha_k \Phi(\|\mathbf{x} - \mathbf{x}_k\|) + \sum_{l=1}^{q} \alpha_{N+l} p_l(\mathbf{x}), \tag{49}$$

where N is the total number of points located in the domain and on the boundary, and $\{\alpha_j\}$, $j = 1, 2, \ldots, N+q$ are the undetermined coefficients. Through collocation, the above

system can be discretized as

$$\sum_{k=1}^{N} \alpha_k \mathbf{L}\Phi(\|\mathbf{x}_i - \mathbf{x}_k\|) + \sum_{l=1}^{q} \alpha_{N+l} \mathbf{L} p_l(\mathbf{x}) = f(u_n(\mathbf{x}_i), v_n(\mathbf{x}_i)), \quad \text{for } \mathbf{x}_i \in \Omega$$
$$\sum_{k=1}^{N} \alpha_k \mathbf{B}\Phi(\|\mathbf{x}_i - \mathbf{x}_k\|) + \sum_{l=1}^{q} \alpha_{N+l} \mathbf{B} p_l(\mathbf{x}) = g(u_n(\mathbf{x}_i), v_n(\mathbf{x}_i)), \quad \text{for } \mathbf{x}_i \in \partial\Omega \quad (50)$$

where n_i represents the number of interior points in Ω.

Since there are additional degrees of freedoms from the polynomial basis, the standard polynomial insolvency constraint [68] must be applied

$$\sum_{i=1}^{N} \alpha_i \mathbf{L} p_l(\mathbf{x}_i) = 0, \quad \text{for } l = 1, \ldots, q \quad (51)$$
$$\sum_{i=1}^{N} \alpha_i \mathbf{B} p_l(\mathbf{x}_i) = 0, \quad \text{for } l = 1, \ldots, q. \quad (52)$$

The system of linear equations (50)–(52) is a square system, where the unknown coefficients $\{\alpha_k\}$ can be obtained by directly solving the system through least squares method. Then the approximate solution w can be obtained from Eq. (49). More details on the numerical simulation can be found in [62].

Now we will test the two-dimensional model (5)–(6) on various scenarios with different coefficients. All numerical results in following sections are performed on an Intel Core 2 2.66 GHz 64 bits computer using MALTAB. The collocation points are distributed uniformly in the domain and on the boundary for simplicity. The number of nodes are examined in which 400 points in square domain and 744 points in the circle domain were chosen. The time step size was tested to ensure the convergence of the results in which we used $\Delta t = 10^{-3}$ in all numerical simulations. The blow up criteria was set to be $\|\mathbf{L}\|_1 < 10^9$ and $\|\mathbf{L}\|_\infty < 10^9$.

Blowup Criteria and Properties

We will first investigate the blowup time and locations regarding different initial conditions and boundary conditions on square domain $[0, \pi]^2$ to test and verify the Theorems 2.2–2.5 and the Corollary 1 in previous section.

The initial conditions used in the following numerical simulations are listed below:

IC1

$$u(x, y, 0) = 0.25(\sin^2(x + y) + \sin^2(x - y)),$$
$$v(x, y, 0) = 0.25(\cos^2(x + y) + \cos^2(x - y)).$$

IC2

$$u(x, y, 0) = 5(\sin^2(x) + \sin^2(y)),$$
$$v(x, y, 0) = 5(\cos^2(x) + \cos^2(y)).$$

IC3

$$u(x, y, 0) = 5(\sin^2(2x) + \sin^2(2y)),$$
$$v(x, y, 0) = 5(\cos^2(2x) + \cos^2(2y)).$$

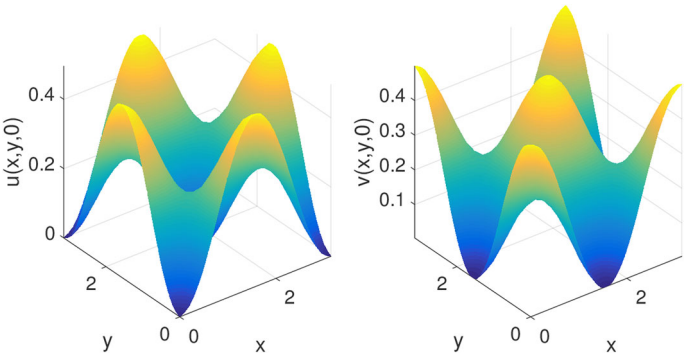

Fig. 1 IC1

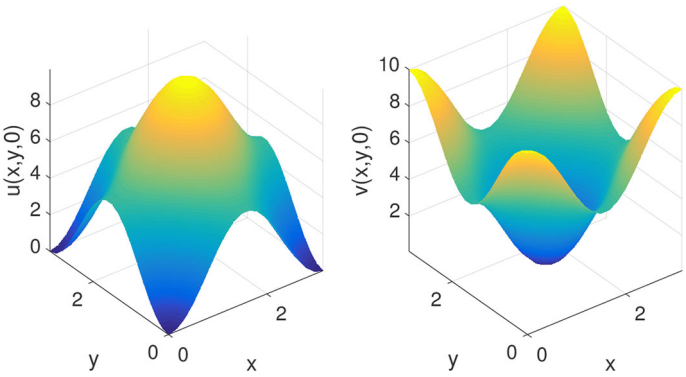

Fig. 2 IC2

IC4

$$u(x, y, 0) = 5(\sin^2(3x) + \sin^2(3y)),$$
$$v(x, y, 0) = 5(\cos^2(3x) + \cos^2(3y)).$$

The profile of the IC1 is shown in Fig. 1, where $\|u_0\|_\infty = \|v_0\|_\infty < 1$. The profile of the IC2 is shown in Fig. 2, where $\|u_0\|_\infty = \|v_0\|_\infty > 1$. The profile of the IC3 is shown in Fig. 3, where $\|u_0\|_\infty = \|v_0\|_\infty > 1$. However, the frequency of the IC3 is doubled compared to the IC2. The profile of the IC4 is shown in Fig. 4, where $\|u_0\|_\infty = \|v_0\|_\infty > 1$. However, the frequency of the IC3 is tripled compared to the IC2. Note $\|u_0\|_\infty = \|v_0\|_\infty$, we use $\mathbf{L}_\infty$ in the following to denote the maximum norm of initial conditions $\|u_0\|_\infty$ and $\|v_0\|_\infty$.

Dirichlet and Neumann BCs

This section tests the solution behavior effected by Dirichlet BCs or Neumann BCs.

As it was proved in earlier sections, the model will blow up in finite time with large initial conditions or the sufficiency conditions of Theorem 2.3 are met. The IC2–IC4 are large initial conditions. The condition of Theorem 2.3 can be met for any $\delta_1 \in (1.999, 2)$ with $\omega_1 = .001$, and $\delta_1 \in (0, 2)$ with $\omega_1 = 3$ in Table 2. The blow up results listed in Table 2 are consistent with Theorems 2.2 and 2.3. From Theorem 2.2, even if conditions of Theorem 2.3 are not

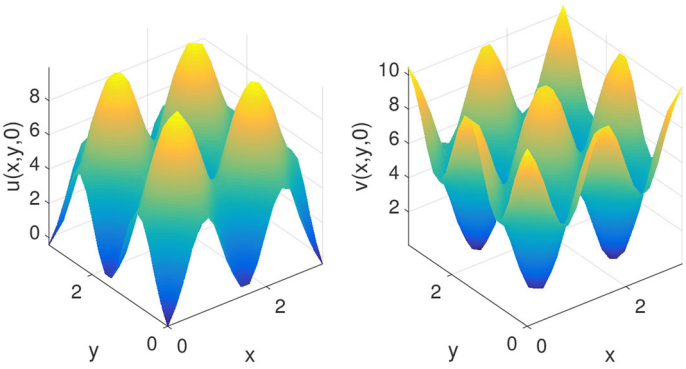

Fig. 3 IC3

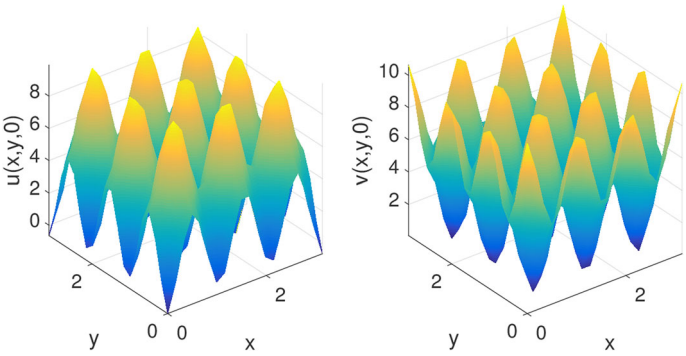

Fig. 4 IC4

Table 2 A summary of theoretical discovery and numerical observations with Dirichlet or Neumann boundary conditions, where $D_u = r = K = \omega = D = d = 1$

BC	IC	D_v	c	ω_1	D_1	IC norm	Theorem 2.3	Blowup
Dirichlet	IC2–IC4	1	2	0.001	1	$\mathbf{L}_\infty > 1$	Met	Yes
	IC2–IC4	1	2	3	1	$\mathbf{L}_\infty > 1$	Met	Yes
	IC1	1	2	3	1	$\mathbf{L}_\infty < 1$	Not met	No
Neumann	IC2–IC4	1	2	0.001	1	$\mathbf{L}_\infty > 1$	Met	Yes
	IC2–IC4	1	2	3	1	$\mathbf{L}_\infty > 1$	Met	Yes
	IC1	1	2	3	1	$\mathbf{L}_\infty < 1$	Not met	No

met, the solutions will also blow up in finite time as long as the initial data are large enough. We will use another example to verify this later in "Mixed boundary conditions".

To test the differences between different blow ups, we plot the solution profile when the blow up criteria met. We also plot the values of v at the blow up locations versus time to represent below up rate. Figures 5 and 6 show blowup profile and blowup rate (profile of v at blowup locations versus time) for Neumann BC case and Dirichlet BC case with the IC2 on the left, the IC3 in the middle and the IC4 on the right. With Neumann BC in Fig. 5, there is no significant difference between blow up times and blow up rates. The number of blow up

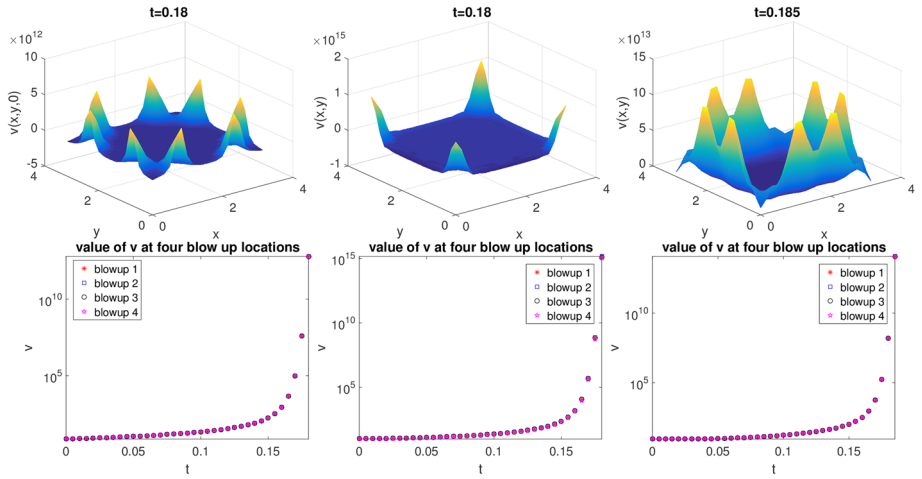

Fig. 5 Blowup profile and blowup rate for Neumann BC case with IC2 on the left, IC3 in the middle and IC4 on the right

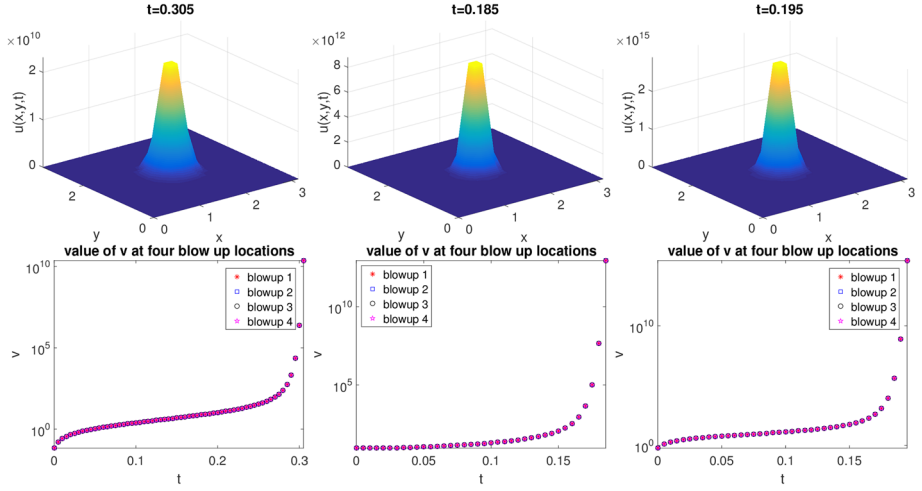

Fig. 6 Blowup profile and blowup rate for Dirichlet BC case with IC2 on the left, IC3 in the middle and IC4 on the right

locations with IC2 and IC4 are similar. With Dirichlet BC in Fig. 6, the blow up time tends to be later and blow up rate is slower if IC2 is used. However, all initial conditions produced blow ups that clustered around the center of the domain.

For the small initial condition IC1, we can not find a $\delta_1 \in (0, c)$ that can satisfy the condition in Theorem 2.3 with $\omega_1 = 3$ in Table 2. Therefore, with the parameters in Table 2, the IC1 meets neither the blow up conditions of Theorem 2.2 nor the Theorem 2.3. Figure 7 shows the convergent solutions of the system when $t = 1$ with small initial condition IC1.

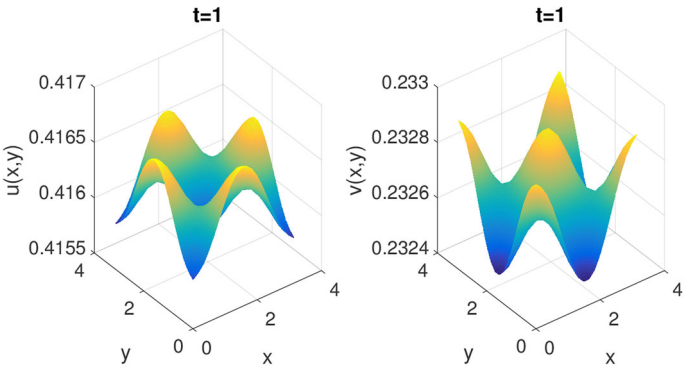

Fig. 7 No blowup cases with Dirichlet BC on the left and Neumann BC on the right with IC1

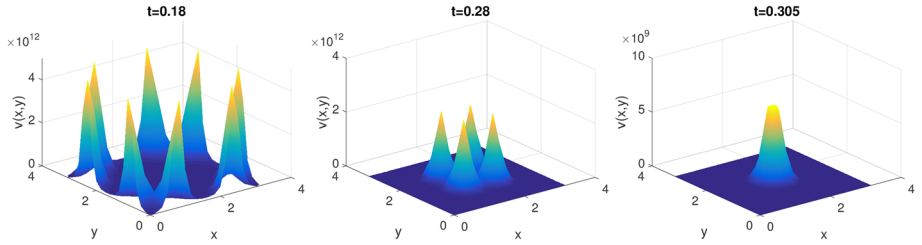

Fig. 8 Blowup with $b = 0$, 10, and 1000 when mixed BCs on a square domain with IC2

Mixed Boundary Conditions

This section exams solution behavior when mixed boundary conditions

$$a_1 u_x + a_2 u_y + bu = 0, \text{ on } \partial\Omega, \tag{53}$$
$$a_1 v_x + a_2 v_y + bv = 0, \text{ on } \partial\Omega \tag{54}$$

are used.

With IC2 under Neumann and mixed boundary condition, we see blow ups in all of our numerical simulation with $w_1 = .001$, see Fig. 8. Since both the conditions for Neumann BC in Theorem 2.3 and conditions for mixed BC in Theorem 2.4 are met, the results are consistent with the theorems in previous section. additionally, numerical simulations suggest that when the coefficient of u in the mixed BCs, b, is bigger, the blowup time tends to be later, and the blowup locations tend to cluster together.

Furthermore, we consider the following initial condition

$$u(x, y, 0) = \gamma(\sin^2(x) + \sin^2(y)),$$
$$v(x, y, 0) = \gamma(\cos^2(x) + \cos^2(y)),$$

with $\gamma = 2$. With the parameters listed in Table 3, where $\omega_1 = 3$, even though the blow up conditions in Theorem 2.3 are not met when $\gamma = 2$, according to Theorem 2.2, the solutions under Neumann boundary conditions will blow up as long as the initial conditions are large. On the left of Fig. 9, we can see that there will be blow ups when $b = 0$, which is consistent with Theorem 2.2 on Neumann BCs. However, there will not be any blowups even with large

Table 3 A summary of theoretical discovery and numerical observations with Neumann and mixed boundary conditions, where $D_u = r = K = \omega = D = d = 1$

IC	D_v	c	ω_1	D_1	IC norm	Conditions in Theorem 2.3	Conditions in Theorem 2.4	Neumann blowup	Mixed blowup
IC2	1	2	0.001	1	$\mathbf{L}_\infty > 1$	Met	Met	Yes	Yes
$\gamma = 2$	1	2	3	1	$\mathbf{L}_\infty > 1$	Not met	Not met	Yes	No
IC1	1	2	3	1	$\mathbf{L}_\infty < 1$	Not met	Not met	No	No
IC1	1	2	0.001	1	$\mathbf{L}_\infty < 1$	Met	Not met	Yes	No

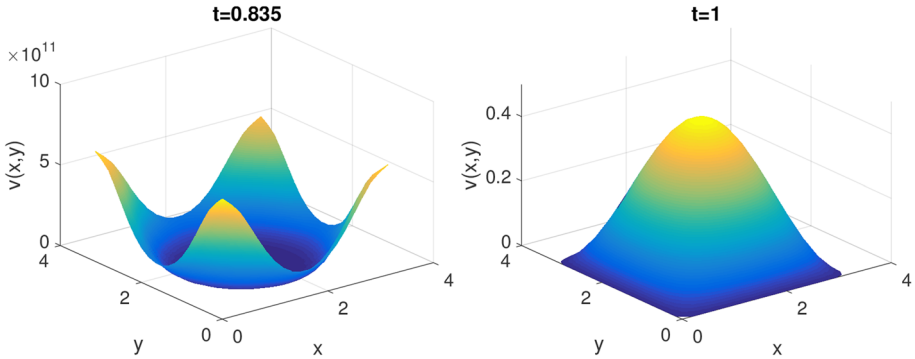

Fig. 9 Blowup with $b = 0$ and no blowup with $b = 10{,}000$ when mixed BCs on a square domain with $\gamma = 2$ is used

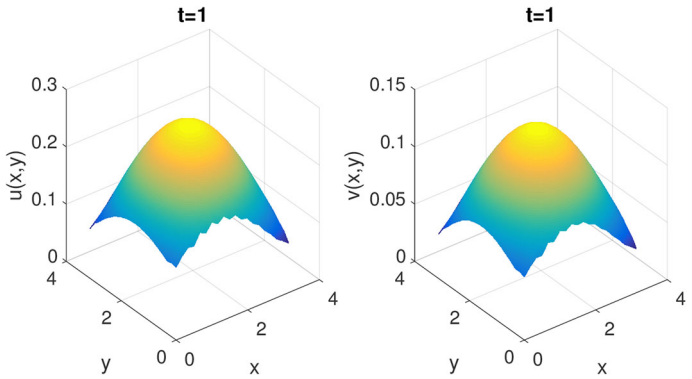

Fig. 10 No blowup case with mixed BCs on a square domain with IC1

initial condition, where $a_1 = a_2 = 1$, $b = 10{,}000$, see the right of Fig 9. This is because the blow up condition $c > \omega_1 / \left(\frac{r-\omega}{r}\right) K + D_1$ for mixed BCs in Theorem 2.4 is not met.

With initial condition IC1, for the two sets of parameters in Table 3, since the initial data is small, the solution with mixed boundary conditions should not blow up from Theorem 2.5. We can see that, in Fig. 10 there is no blow up shown in the profile of the solutions with $a_1 = a_2 = b = 1$, $\omega_1 = 3$ when $t = 1$. When $\omega_1 = .001$, because the conditions of Theorem 2.3 are met, the solutions blow up under Neumann BC. From Table 3, we can see the mixed boundary conditions can provide a "damping" effect.

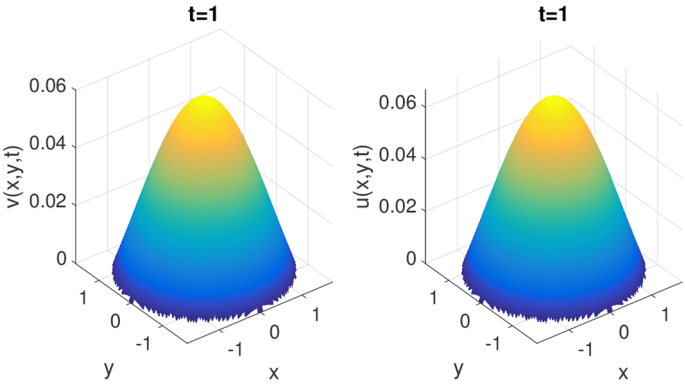

Fig. 11 No blowup case with Dirichlet BC on a circle domain

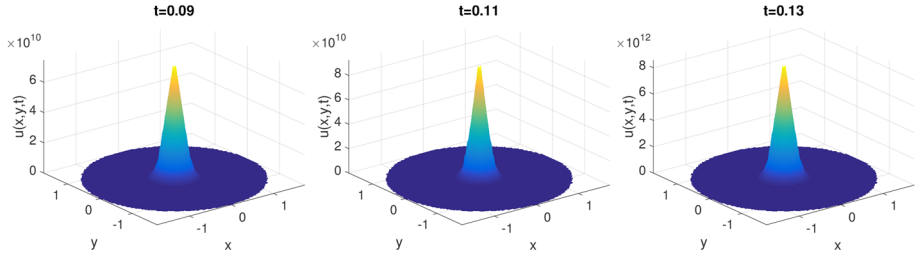

Fig. 12 Blowup case with Dirichlet BC on a circle domain with IC2 on the left, IC3 in the middle, and IC4 on the right. The parameters are $c = 2$, $\omega_1 = 0.001$, $D_1 = 1$, $N_t = 200$, order of the polyharmonic splines is $m = 2$, and the order of polynomials is 1

Circle Domain

This section focuses on solution behavior to the model on a circle domain in 2D instead of square domain. Our goal is to use numerical simulation to predict what would happen to the PDE model, if the domain is a circle instead of a square.

- Dirichlet BC: Figure 11 shows the numerical solution with Dirichlet BC and IC1, $\omega_1 = 3$. There is no blowup. This is consistent with the results on square domains.
  Blowup cases with Dirichlet BC on a circle domain are shown in Fig. 12 for IC2 on the left, IC3 in the middle, and IC4 on the right. The parameters are $c = 2$, $\omega_1 = 0.001$, $D_1 = 1$, $N_t = 200$, order of the polyharmonic splines is $m = 2$, and the order of polynomials is 1.
- Neumann BC:
  - IC1: In the circle domain with Neumann BCs and IC1, the original set of parameters chosen for the square domain ($c = 2, \omega_1 = 3, D_1 = 1$) does not leads to an equilibrium solution. That says, we still have a blowup, except if we chose a bigger ω_1, such as $\omega_1 = 10$, see Fig. 13.
  - IC2, IC3 and IC4: Blowup cases with Neumann BC on a circle domain are shown in Fig. 14 with IC2 on the left, IC3 in the middle, and IC4 on the right. The parameters are $c = 2$, $\omega_1 = 0.001$, $D_1 = 1$, $N_t = 200$, order of the polyharmonic splines is $k = 2$, and the order of polynomials is 1.

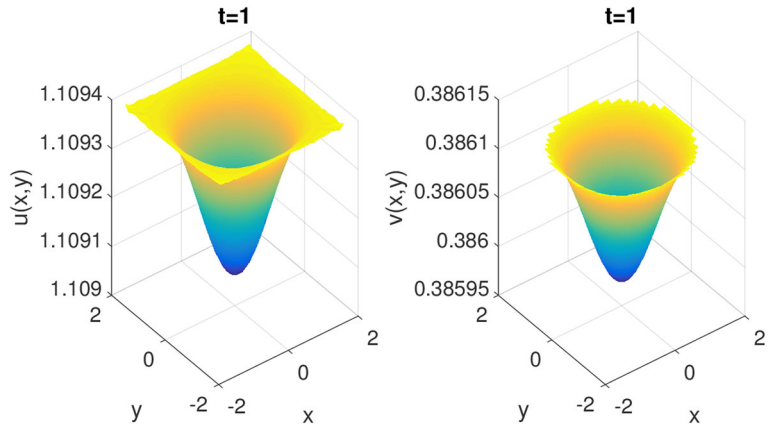

Fig. 13 No blowup case with Neumann BC on a circle domain with IC1. The parameters are $c = 2, \omega_1 = 10$, $D_1 = 1$, $N_t = 200$, order of the polyharmonic splines is $m = 2$, and the order of polynomials is 1

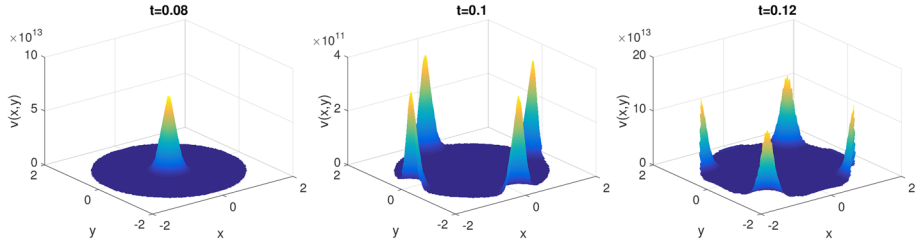

Fig. 14 Blowup case with Neumann BC on a circle domain with IC2 on the left, IC3 in the middle, and IC4 on the right. The parameters are $c = 2, \omega_1 = 0.001$, $D_1 = 1$, $N_t = 200$, order of the polyharmonic splines is $m = 2$, and the order of polynomials is 1

- Mixed BC: Blowup case with mixed BC on a square domain with IC2 with $a_1 = a_2 = 1$ is shown in Fig. 15 on the left, $b = 1$, and no blowup case with mixed BC and IC2 with coefficient $a_1 = a_2 = 1$ and $b = 10{,}000$ on the right. The parameters are $c = 3$, $\omega_1 = 1$, $D_1 = 1$, $N_t = 200$, order of the polyharmonic splines is $m = 2$, and the order of polynomials is 1. L^1 norm is used as the criteria of blowup. In this situation, even though the sufficiency conditions of Theorem 2.3 are met, the solutions are bounded when b is chosen large enough, which verifies the Corollary 1.

Discussion

In the context of blowup we see from our theoretical and numerical results, that mixed boundary conditions prevent blow-up/excessive concentrations of the invasive. With initial condition IC3, there is no blowup, see Fig. 10. Also we see with the mixed BCs, when b, is bigger, the blowup time tends to be later, and the blowup locations tend to cluster. From Fig. 9, we can see that there will be blow-up when $b = 0$, but no blow-up even with large initial conditions γ, where $a_1 = a_2 = 1, b = 10{,}000$ are chosen, see the right of Fig. 9. This tells us that if efficient mechanisms are in place for sufficient number of individuals to cross the boundary of the physical domain when encountering it [69], high local concentrations

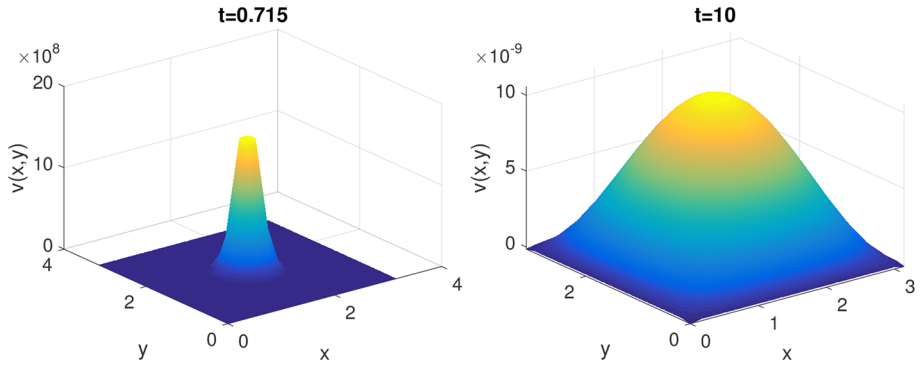

Fig. 15 Blowup case with mixed BC on a square domain with IC2 with $a_1 = a_2 = 1$ on the left, $b = 1$, and no blowup case with mixed BC and IC2 with coefficient 1 and $b = 10{,}000$ on the right. The parameters are $c = 3, \omega_1 = 1, D_1 = 1, N_t = 200$, order of the polyharmonic splines is $m = 2$, and the order of polynomials is 1. l_1 norm is used as the criteria of blowup

will be prevented. This result is also rigorously proved via Theorem 2.5, and Corollary 1. Corollary 1 in part also tells us that if we have an exploding population in a region, it can be effectively controlled, *solely* via manipulation of the boundary. Thus the invasive does not have to be engaged in the interior of the region, say via chemical control. More importantly since current government policy, does not permit the harvesting of pythons in the actual park area, any action in the interior of the domain is actually *impossible*. Thus the python population can grow unchecked there. Our methods show that facilitating flow of some of the pythons from the interior of the park to outside it, will check the python population overall. How then does one facilitate such movement?

Note, a *corridor* is an area of habitat connecting populations separated by various activities, allowing an exchange of individuals of a species [41]. From an ecological point of view, this tell us that if we have efficient corridor design, then this can prevent high local concentrations of invasive species. This is debated and there is much regulation from environmental agencies, which often want to keep an invasive species contained locally, as opposed to letting it spread due to obvious negative effects [69]. However, if efficient chemical control is used at *specific* target cites, such as at these corridors, then we could have an efficient control in place. Furthermore, these sites would also lye outside the park boundaries, and so python removal here (by chemical means or mechanical) would be allowable by law.

Also, there is much evidence that predators are attracted to sites of prey refuges (regions where prey are protected) [70]. Natural examples are seen with snakes crowding near bat caves, and weasel activity heightened near vole refuges [71]. There is also experimental evidence of this, as seen via tracking ocelots hunting for agouti [70]. This tells us that it would be interesting, given our results to combine refuge design, with corridor design. That is one might place refuges, at the ends of corridors, as a means to attract the invasive out of the domain in question (or the one where blow-up/high local concentration is seen), and towards the refuge. Then one can use chemical control at these cites. Thus as in [24] we reaffirm that the optimal placement of a damping mechanism becomes most important. That is managers can use refuges to draw out quantities of an invasive species from a habitat where there are excessively high concentrations of them, facilitating their passage via corridors, and then use chemical control in localised regions, for maximum impact. To this end, given that we want to use chemical controls in a certain domain, the blow-up results we obtain are very useful.

Again, we see irrespective of initial condition, blow-up often occurs at the centre. This give us a spatial target, for the chemical control. This is much akin to disease models, where the appropriate strategy is to vaccinate at certain key areas [72].

In the current manuscript we have also investigated the effect of changing the shape of the physical domain, on the blow-up dynamics. This gives us some intuitions, about how landscape might effect population explosion. What we see is that in a circle domain, there is no obvious advantage to blow-up removal. That is most blow-up results are consistent, with the square domain.

Conclusion

In the current manuscript, we investigate a spatially explicit predator–prey model, where the predator population has the potential to explode/blow-up in finite time. This is interpreted as perhaps an invasive species, going out of control or a defoliator or pest outbreaking. This is formalized by equating:

$$\text{finite time blow-up} = uncontrollable \text{ and } unmanageable \text{ population level}, \tag{55}$$

where, the blow-up time T^* is viewed as the "disaster" time, for the ecosystem. We next consider damping mechanisms *different* from classical chemical and biological control. We focus on mixed boundary conditions as well as pure Neumann boundary conditions. The following conclusions can be made:

- The mixed (in particular Robin type) boundary conditions are shown to provide a "damping" effect.
- The PDE system blowup occurs differently in square domains than in circular domains.

Note numerically, we have only considered equations on square domains and circle domains. However, as landscapes change, from ecosystem to ecosystem, it is worth considering domains of different shapes, and their effect on subsequent population explosion. This will make for interesting future research.

Our ultimate goal is to highlight certain workable scenarios that might be implemented as control policy by managers and practitioners. Often a conservation biologist/manager has a variety of choices with control mechanisms, and needs to choose the best possible one, or the best combination of these [73,74]. For example, the population of many bird species have declined globally [75], due to predation by invasive predators [10]. Conservation biologists have used predator exclosure methods with success [75,76], but are often faced with a decision of the most *cost effective* combination of measures such as exclosure fencing versus nest cover to use [73]. Thus it would make for interesting future work to investigate models, that incorporate a combination of corridors (mixed boundary conditions) coupled with chemical control, and work out optimal scenarios to keep the invasive/pest density low, or drive it towards extinction. These directions essentially warrant investigating a spatially dependent b, that is $b = b(x)$. The other interesting future direction is to consider time dependent/stochastic parameters, such as in [50]. For starters one may consider the sexual reproduction rate to be time dependent $c = c(t)$, or time dependent and stochastic $c = c(\omega, t)$. The effect of this on the blow-up dynamics could be investigated. It will be interesting to note if the results differ significantly from the constant parameter case.

Another future direction is to formulate this combination of measures so as to optimise (or minimise) the costs associated with implementing them. This is the control theory approach.

Such an approach has been taken in recent works that look at optimal introduction of genetically modified organisms for the biological control of invasive fish populations [77]. An optimal control formulation of the problem would make an interesting future direction. Most interestingly, it would also be very interesting in the future to consider deriving optimal conditions on the spatially dependent b, that is $b = b(x)$ coefficient in question, to see if an appropriate function blows-up or not, depending on how b is manipulated. This would have far reaching consequences in actual practice for eco-system managers wishing to use *solely* the boundary as a tool for population control.

All in all, we hope that our results will encourage ecosystem managers, practitioners and government entities to invest in, and further investigate sound ecosystem engineering methodologies such as efficient corridor design as an environmentally friendly method, and boundary manipulation techniques, to prevent excessively high local concentrations of invasive species. This in turn will help boost native biodiversity and restore ailing eco-systems.

Acknowledgements We would like to acknowledge valuable comments from the referees that helped us greatly improve the overall quality of the manuscript.

References

1. Pimentel, D., Zuniga, R., Morrison, D.: Update on the environmental and economic costs associated with alien-invasive species in the United States. Ecol. Econ. **52**(3), 273–288 (2005)
2. Simberloff, D.: Introduced species: the threat to biodiversity and what can be done. http://www.actionbioscience.org/biodiversity/simberloff.html . Accessed Dec 2000
3. Arim, M., Abades, S., Neill, P., Lima, M., Marquet, P.: Spread dynamics of invasive species. Proc. Natl. Acad. Sci. **103**(2), 374–378 (2006)
4. Averill, I., Lou, Y.: On several conjectures from evolution of dispersal. J. Biol. Dyn. **6**(2), 117–130 (2012)
5. Bampfylde, C.J., Lewis, M.A.: Biological control through intraguild predation: case studies in pest control, invasive species and range expansion. Bull. Math. Biol. **69**, 1031–1066 (2007)
6. Clark, J.S., Lewis, M., Horvath, L.: Invasion by extremes: population spread with variation in dispersal and reproduction. Am. Nat. **157**(5), 537–554 (2001)
7. Lou, Y., Munther, D.: Dynamics of a three species competition model. Discrete Contin. Dyn. Syst. A **32**, 3099–3131 (2012)
8. Okubo, A., Maini, P.K., Williamson, M.H., Murray, J.D.: On the spatial spread of the grey squirrel in Britain. Proc. R. Soc. Lond. Ser. B **238**, 113–125 (1989)
9. Shigesada, N., Kawasaki, K.: Biological Invasions: Theory and Practice. Oxford University Press, Oxford (1997)
10. Dorcas, M.E., Willson, J.D., Reed, R.N., Snow, R.W., Rochford, M.R., Miller, M.A., Mehsaka Jr., W.E., Andreadis, P.T., Mazzotti, F.J., Romagosa, C.M., Hart, K.M.: Severe mammal declines coincide with proliferation of invasive Burmese pythons in Everglades National Park. Proc. Natl. Acad. Sci. **109**, 2418–2422 (2012)
11. Schofield, P., Loftus, W.: Nonnative fishes in Florida freshwaters: a literature review and synthesis. Rev. Fish. Biol. Fish. **25**(1), 117–145 (2015)
12. Hood, J.: Asian carp: State's fish kill in Chicago sanitary and ship canal yield only 1 Asian carp. (2009) http://www.articles.chicagotribune.com. Accessed 26 June 2017
13. Blinder, A.: Aimed at Zika Mosquitoes, spray kills millions of honeybees, New York Times, Sept 1. http://www.nytimes.com/2016/09/02/us/south-carolina-pesticide-kills-bees.html?_r=0 (2016)
14. Wedekind, C.: Demographic and genetic consequences of disturbed sex determination. Phil. Trans. R. Soc. B **372**(1729), 20160326 (2017)
15. Wedekind, C.: Managing population sex ratios in conservation practice:how and why?. In: Topics in Conservation Biology. InTech (2012)
16. Crossland, M.R., Haramura, T., Salim, A.A., Capon, R.J., Shine, R.: Exploiting intraspecific competitive mechanisms to control invasive cane toads. Proc. Biol. Sci. **279**(1742), 3436–3442 (2012)
17. Berryman, A et al.: The theory and classification of outbreaks. In: Insect Outbreaks, pp 3–30. Academic Press, Inc., (1987)

18. Ludwig, D., Holling, C.: Qualitative analysis of insect outbreak systems: the spruce budworm and forest. J. Anim. Ecol. **47**(1), 315–332 (1978)
19. Diez, J.M., D'Antonio, C.M., Dukes, J.S., Grosholz, E.D., Olden, J.D., Sorte, C.J., Jones, S.J.: Will extreme climatic events facilitate biological invasions? Front. Ecol. Environ. **10**(5), 249–257 (2012)
20. Van Driesche, R., Bellows, T.: Biological Control. Kluwer Academic Publishers, Massachusetts (1996)
21. Parshad, R.D., Abderrahmanne, H., Upadhyay, R.K., Kumari, N.: Finite time blowup in a realistic food chain model. ISRN Biomath. **2013**, 1–12 (2013). (Article ID 424062)
22. Parshad, R.D., Basheer, A.: "A note on periodic solutions of a three-species food chain model" [Applied Math E-Notes, 9 (2009), 47–54]. Appl. Math. E Notes **16**, 45–55 (2016)
23. Parshad, R.D., Kumari, N., Kouachi, S.: A remark on "Study of a Leslie–Gower-type tritrophic population model" [Chaos, Solitons and Fractals 14 (2002) 1275–1293]. Chaos Solitons Fractals **71**, 22–28 (2015)
24. Parshad, R.D., Qansah, E., Black, K., Beauregard, M.: Biological control via "ecological" damping: an approach that attenuates non-target effects. Math. Biosci. **273**, 23–44 (2016)
25. Parshad, R., Upadhyay, R.K., Mishra, S., Tiwari, S., Sharma, S.: On the explosive instability in a three species food chain model with modified Holling type IV functional response. Math. Methods Appl. Sci. (2017). https://doi.org/10.1002/mma.4419 **(Appeared online May 3rd)**
26. Parshad, R.D., Kouachi, S., Kumari, N.: A comment on "Mathematical study of a Leslie–Gower type tritrophic population model in a polluted environment" [Modeling in Earth Systems and Environment 2 (2016) 1–11.]. Model. Earth Syst. Environ. **2**(2), 1–5 (2016)
27. Quittner, P., Souplet, P.: Superlinear Parabolic Problems: Blow-up, Global Existence and Steady States. Birkhauser, Basel (2007)
28. Straughan, B.: Explosive Instabilities in Mechanics. Springer, Heidelberg (1998)
29. Kim, K., Lin, Z.: Blowup in a three species cooperating model. Appl. Math. Lett. **17**, 89–94 (2004)
30. Lou, Y., Nagylaki, T., Ni, W.: On diffusion induced blowups in a mutualistic model. Nonlinear Anal. **45**, 329–342 (2001)
31. Hillen, T., Painter, K.: A users guide to PDE models for chemotaxis. J. Math. Biol. **57**, 183–217 (2009)
32. Grinn, L., Hermann, P., Korotayev, A., Tausch, A.: History & Mathematics: Processes and Models of Global Dynamics. 'Uchitel' Publishing House, Volgograd (2010)
33. Parshad, R.D., Qansah, E., Beauregard, M., Kouachi, S.: On, "small" data blow-up in a three species food chain model. Comput. Math. Appl. **73**(4), 576–587 (2017)
34. Parshad, R.D., Bhowmick, S., Quansah, E., Basheer, A., Upadhyay, R.K.: Predator interference effects on biological control: the paradox of the generalist predator revisited. Commun. Nonlinear Sci. Numer. Simul. **39**, 169–84 (2016)
35. Quansah, E., Parshad, R.D., Mondal, S.: Cold induced mortality of the Burmese Python: an explanation via stochastic analysis. Physica A **467**(1), 356–364 (2017)
36. Parshad, R.D., Basheer, A., Jana, D., Tripathi, J.: Do prey handling predators really matter: subtle effects of a Crowley-Martin functional response. Chaos Solitons Fractals **103**, 410–421 (2017)
37. Shang, Y.: Finite-time consensus for multi-agent systems with fixed topologies. Int J Syst Sci **43**(3), 499–506 (2012)
38. Shang, Y., Ye, Y.: Fixed-time group tracking control with unknown inherent nonlinear dynamics. IEEE Access **5**, 12833–12842 (2017)
39. "United States of America, North America". UNEP. World Database on Protected Areas. 2015–05-02. Retrieved 2015–05-02
40. Cantrell, R., Cosner, C.: Spatial Ecology via Reaction Diffusion Equations. Wiley, Chichester (2003)
41. Kindlmann, P., Burel, F.: Connectivity measures: a review. Landsc. Ecol. **23**, 879–890 (2008)
42. Upadhyay, R.K., Agrawal, R.: Dynamics and responses of a predatorprey system with competitive interference and time delay. Nonlinear Dyn. **83**(1–2), 821–837 (2016)
43. Beddington, J.: Mutual interference between parasites or predators and its effect on searching efficiency. J. Anim. Ecol. **44**, 331–340 (1975)
44. Hassell, M.P.: Mutual interference between searching insect parasites. J. Anim. Ecol. **40**, 473–486 (1971)
45. Rogers, D.J., Hassell, M.P.: General models for insect parasite and predator searching behaviour: interference. J. Anim. Ecol. **43**, 239–253 (1974)
46. Hassell, M.: Density dependence in single species population. J. Anim. Ecol. **44**, 283–295 (1975)
47. Allaby, M.: A Dictionary of Ecology. Oxford University Press, Oxford (2010)
48. Freedman, H.I., Rao, V.S.H.: The trade-off between mutual interferences and time lag in predator prey systems. Bull. Math. Biol. **45**, 991–1004 (1983)
49. Berec, L.: Impacts of foraging facilitation among predators on predatorprey dynamics. Bull. Math. Biol. **72**, 94–121 (2010)
50. Shang, Y.: The limit behavior of a stochastic logistic model with individual time-dependent rates. J. Math. **2013**, 1–7 (2013)

51. Li, B., Liao, C.H., Zhang, X.D., Chen, H.L., Wang, Q., Chen, Z.Y., Cheng, X.L.: Spartina alterniflora invasions in the Yangtze River estuary, China: an overview of current status and ecosystem effects. Ecol. Eng. **35**(4), 511–520 (2009)
52. Payne, L.E., Schaefer, P.W.: Blow-up in parabolic problems under Robin boundary conditions. Appl. Anal. **87**, 699–707 (2008)
53. Sell, G., You, Y.: "Dynamics of evolutionary equations". Applied Mathematical Sciences, vol. 143, 2nd edn. Springer, New York (2002)
54. Wei, J., Winter, M.: Mathematical Aspects of Pattern Formation in Biological Systems, vol. 189. Springer Science & Business Media, Berlin (2013)
55. Zerroukat, M., Power, H., Chen, C.S.: A numerical method for heat transfer problems using collocation and radial basis functions. Int. J. Numer. Methods Eng. **42**, 1263–1278 (1998)
56. Sarler, B., Gobin, D., Goyeau, B., Perko, J., Power, H.: Natural convection in porous media-dual reciprocity boundary element method solution of the Darcy model. Int. J. Numer. Methods Fluids **33**, 279–312 (2000)
57. Chantasiriwan, S.: Performance of multiquadric collocation method in solving liddriven cavity flow problem with low reynolds number. Comput. Model. Eng. Sci. **15**, 137–146 (2006)
58. Yao, G., Yu, Z.: A localized meshless approach for modeling spatial-temporal calcium dynamics in ventricular myocytes. Int. J. Numer. Methods Biomed. Eng. **28**(2), 187–204 (2012)
59. Chen, C.S., Fan, C.M., Wen, P.H.: The method of particular solutions for solving certain partial differential equations. Numer. Methods Part. Differ. Equ. **28**, 506–522 (2012)
60. Yao, G.: Local radial basis function methods for solving partial differential equations. The University of Southern Mississippi (2010)
61. Lamichhane, A.R., Chen, C.S.: The closed-form particular solutions for Laplace and biharmonic operators using a Gaussian function. Appl. Math. Lett. **46**, 50–6 (2015)
62. Yao, G., Zheng, H., Chen, C.S.: A modified method of approximate particular solutions for solving linear and nonlinear PDEs. Numer. Methods Partial Differ. Equ. **33**(6), 1839–1858 (2017)
63. Chen, C.S., Fan, C.M., Wen, P.H.: The method of particular solutions for solving elliptic problems with variable coefficients. Int. J. Comput. Methods **8**, 545–559 (2011)
64. Wen, P.H., Chen, C.S.: The method of particular solutions for solving scalar wave equations. Int. J. Numer. Methods Biomed. Eng. **26**(12), 1878–89 (2010)
65. Bustamante, C.A., Power, H., Sua, Y.H., Florez, W.F.: A global meshless collocation particular solution method (integrated Radial Basis Function) for two-dimensional Stokes flow problems. Appl. Math. Modell. **37**(6), 4538–4547 (2013)
66. Reutskiy, S.Y.: Method of particular solutions for nonlinear Poisson-type equations in irregular domains. Eng. Anal. Bound. Elem. **37**(2), 401–408 (2013)
67. Iske, A.: On the stability of polyharmonic spline reconstruction. In: Conference Proceedings of Sampling Theory and Applications (SampTA2011)
68. Chen, C.S., Hon, Y.C., Schaback, R.A.: Scientific computing with radial basis functions. Tech. Rep., Department of Mathematics, University of Southern Mississippi, Hattiesburg, MS 39406, USA, preprint (2005)
69. Resasco, J., et al.: Landscape corridors can increase invasion by an exotic species and reduce diversity of native species. Ecology **95**(8), 2033–2039 (2014)
70. Emsens, W., Hirch, B., Kays, R., Jansen, P.: Prey refuges as predator hotspots: ocelot (*Leopardus pardalis*) attraction to agouti (*Dasyprocta punctata*) dens. Acta Theriol. **59**(2), 257–262 (2014)
71. Ylonen, H., Sundell, J., Tiilikainen, R., Eccard, J., Horne, T.: Weasels (Mustela nivalis nivalis) preference for olfactory cues of the vole (Clethrionomys glareolus). Ecology **84**, 1447–1452 (2003)
72. McCarthy, K.A., Chabot-Couture, G., Shuaib, F.: A spatial model of Wild Poliovirus Type 1 in Kano State, Nigeria: calibration and assessment of elimination probability. BMC Infect. Dis. **16**(1), 521 (2016)
73. Robinson, O., Fefferman, N., Lockwood, J.: How to effectively manage invasive predators to protect their native prey. Biol. Conserv. **165**, 146–153 (2013)
74. Hobbs, R., Hallett, L., Ehrlich, P., Mooney, H.: intervention ecology: applying ecological science in the twenty-first century. BioScience **61**(6), 1–9 (2011)
75. Isaksson, D., Wallander, J., Larsson, M.: Managing predation on ground-nesting birds: the effectiveness of nest exclosures. Biol. Conserv. **136**, 136–142 (2007)
76. Ivan, J.S., Murphy, R.K.: What preys on piping plover eggs and chicks? Wildl. Soc. Bull. **33**(1), 113119 (2005)
77. Kelly, Jr., M, R., Wang, X.: The optimal implementation of the trojan y chromosome eradication strategy of an invasive species. J. Biol. Syst. **25**, 1–20 (2017)